

N O T I C E

THIS DOCUMENT HAS BEEN REPRODUCED FROM
MICROFICHE. ALTHOUGH IT IS RECOGNIZED THAT
CERTAIN PORTIONS ARE ILLEGIBLE, IT IS BEING RELEASED
IN THE INTEREST OF MAKING AVAILABLE AS MUCH
INFORMATION AS POSSIBLE

Voltage Gradients in Solar Array Cavities as Possible Breakdown Sites in Spacecraft-Charging-Induced Discharges

(NASA-TM-82710) VOLTAGE GRADIENTS IN SOLAR
ARRAY CAVITIES AS POSSIBLE BREAKDOWN SITES
IN SPACECRAFT-CHARGING-INDUCED DISCHARGES
(NASA) 10 p HC A02/MF A01 CSCL 10B

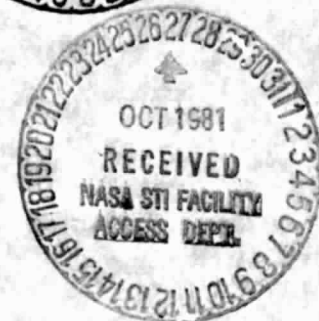
N82-11107

Unclas

G3/18

27665

N. John Stevens, Hilton E. Mills
and Lisa Orange
*Lewis Research Center
Cleveland, Ohio*



Prepared for the
Annual Conference on Nuclear and Space Radiation Effects
sponsored by the Institute of Electrical and Electronic Engineers
Seattle, Washington, July 21-24, 1981

NASA

VOLTAGE GRADIENTS IN SOLAR ARRAY CAVITIES AS POSSIBLE BREAKDOWN SITES IN SPACECRAFT-CHARGING-INDUCED DISCHARGES

by N. John Stevens, Hilton E. Mills and Lisa Orange

National Aeronautics and Space Administration
Lewis Research Center
Cleveland, Ohio 44135

Summary

A possible explanation for environmentally-induced discharges on geosynchronous satellites exists in the electric fields formed in the cavities between solar cells - the small gaps formed by the cover slides, solar cells, metallic interconnects and insulating substrate. When exposed to a substorm environment, the cover slides become less negatively charged than the spacecraft ground. Hence, it is possible for metallic surfaces (usually silver mesh) to be at a negative potential in a cavity that has a "positive" surface above it. If the resultant electric field becomes large enough, then the interconnect could emit electrons (probably by field emission) which could be accelerated to space by the positive voltage on the covers. An experimental study was conducted using a small solar array segment in which the interconnect potential was controlled by a power supply while the cover slides were irradiated by monoenergetic electrons. It was found that discharges could be triggered when the interconnect potential became at least 500 volts negative with respect to the cover slides. Analytical modeling of satellites exposed to substorm environments indicates that such gradients are possible. Therefore, it appears that this trigger mechanism for discharges is possible. Details of the experiment and modeling study are presented.

Introduction

In the early seventies, geosynchronous satellites began recording spurious electronic switching anomalies.¹ It was shown that such satellites could be charged by the geomagnetic substorm environment to significant negative potentials (relative to space).^{2,3} The original assumption made was that the dark or shaded insulator surfaces would be differentially charged (relative to the sunlit or structure potential) to a point where discharges could occur. The electromagnetic pulse from the discharge would couple into the electrical harness and generate a pseudo-command pulse triggering the low level logic circuits or disrupting telemetry.⁴ Based on the ATS-5 and 6 ground potential measurements during substorms, differential voltages of 10 to 20 kV were believed to be possible.^{2,3,5}

Ground simulation tests were run on various satellite insulator surfaces usually with monoenergetic electron beams.⁶⁻⁹ These tests usually produced spectacular, visible discharge patterns on the test surfaces. The differential voltage thresholds to initiate these discharges were between 8 and 15 kV.⁹ Therefore, it was felt that such discharges could occur in space conditions and studies continued to characterize discharge transients as functions of storm intensity and surface area.^{8,10}

Recent space data¹¹ and spacecraft analytical modeling studies¹²⁻¹⁴ have indicated that differential voltages built up on satellites are considerably less than those originally assumed. The shaded surfaces are not independently charged from the sunlit surfaces. As the shaded surfaces start to charge electric fields develop that surround the satellite, building up potential barriers that limit photoemission.¹⁵ Hence, differential charging is

limited to values of -2 to -4 kV. Ground tests indicate that, at these differential voltages, there should be no discharges. Yet, space data does indicate that discharges occur.¹⁶⁻¹⁸ Therefore, different mechanisms have to be postulated for environmentally-induced discharges.

One of the first possible mechanisms suggested is the buried-charge-induced breakdown.^{19,20} This concept postulates that the higher energy particles found in substorm environments can be buried within the insulation surfaces while the exterior potential is maintained at low negative voltages by photoemission or secondary emission. Breakdowns can then occur between the charged layer and surface. Another possible mechanism is that of a slightly charged satellite breaking down to space.²¹⁻²³

Another discharge mechanism is possible; that due to inverted voltage gradients. Previous analytical studies have indicated that solar array covers could charge negatively with respect to space, but to voltages that were positive with respect to spacecraft ground.^{13,14} This can result in strong electric fields within limited space and lead to possible discharges. This concept was proposed and demonstrated previously using electron beams and ultraviolet lamps.²⁴ Breakdowns were obtained at inferred differential voltages of about 1000 volts. In this study the concept is further evaluated using low energy low flux electron beams and the results compared to NASCAP predictions.

Solar Array Positive Voltage Gradient Evaluation

Basic Concept

Solar arrays are constructed with numerous individual solar cells arranged in series-parallel circuits. In the standard construction configuration the solar cells (usually 2x2 cm) are connected in series by a silver mesh interconnect bent to allow for expansion (see Fig. 1(a)). Over each cell is placed a cover slide which is either fused silica or cerium doped microsheet, 0.15 - 0.25 mm thick. Anti-reflective coatings, such as magnesium fluoride are usually placed on the exterior of the covers. This method of construction leaves small gaps between the cells - on the order of 1 to 2 mm - which expose the interconnects to the environment. The whole array sets on an insulation sheet which can be attached to a honeycomb substrate.

In space, the satellite surfaces are exposed to charged-particle fluxes and sunlight. All surfaces will come to an equilibrium voltage such that the net current to that surface is zero. The currents involved are the incident particle currents, the photoemitted current (in sunlight), the secondary emitted currents, backscattered currents, leakage currents and stored charges in capacitors. In a substorm environment, the incident charged-particle currents increase causing an increase in surface voltage (usually negative). The spacecraft ground potential (relative to space plasma potential) is determined by the total current balance on all the exposed metallic areas of the satellite. The interconnects will be at a voltage dependent upon their location in the array. This value will be close to spacecraft ground since operating voltages on satellites tend to be modest, e.g., ≤ 60 volts.

The cover slides on the solar array will also come into an equilibrium potential (relative to space plasma potential) such that the net current to these surfaces is zero. Modeling studies of satellites indicate that solar array voltages are significantly less negative than the structures.^{13,14,25}

This configuration results in a very small gap having a bent metallic surface which is negative with respect to the voltages on the covers (see Fig. 1(b)). In this gap, it is possible to have the interconnect emit electrons by field emission and have the electrons accelerated out of the gap to space - to trigger a discharge pulse. The emission of electrons can collapse the field causing the discharge to cease. This is the concept that is evaluated in this paper.

Experimental Results

The experimental arrangement for these tests is shown in Fig. 2. The tests were conducted in a stainless steel bell jar vacuum system. The electron flood gun is capable of producing a broad, monoenergetic electron beam in which the energy can be set at any value between -1 and -10 kV by an external power supply. Beam current densities at the target plane were set at approximately 1 nA/cm prior to starting each charging test.

The test specimen was a small solar array segment originally built for the SPHINX satellite²⁷ (Fig. 2(b)). It consisted of twenty-four 2x2 cm solar cells connected in series. The cells were mounted on a Kapton sheet which, in turn, was mounted on a fiberglass board. The solar cells were flight quality, the interconnects, silver mesh and the cover slides, fused silica.

The tests consisted of irradiating this segment with a monoenergetic electron beam (at a specified energy) while controlling the interconnect voltage with a power supply. The principal measurement was obtained by sweeping a surface voltage probe (TREK) across one of the middle rows of the array. Tests were run with electron beam energies of -2, -4 and -6 keV and applied positive and negative bias voltages to the interconnects that were set at values from 0 to at least the beam voltage value. The following paragraphs will concentrate on the negative bias voltage results.

Typical surface voltage profiles across the central three solar cells of the middle row are shown in Fig. 3 for tests run with 4 keV electron beams. The surface voltage profile obtained with the interconnects at zero volts (grounded) are shown in Fig. 3(a). This is a typical result with the cover slide potential varying between -100 and -200 volts depending on the cell location. These are equilibrium surface voltages and show the effect of high secondary yield magnesium fluoride anti-reflection coating.²⁶ Plain silica surfaces would have a surface voltage considerably higher.⁶ Note that the interconnects are positive with respect to the cover slides. The surface voltages of the first and sixth solar cell of this row have not been shown since their potentials are distorted by the Kapton insulation sheet.

When negative bias voltages are applied, surface voltage characteristics change: voltages on the glass surfaces become more negative. The interconnect potentials, which were originally positive with respect to the covers, eventually become equal to the cover surface voltage as the applied negative bias voltage increases. For larger bias voltages, the interconnect potentials become negative with respect to the glass. As the bias voltage is increased further, the interconnect potentials become increasingly larger while remaining confined essentially to the gap region. These results are shown in Fig. 3(b). The graphs represent equilibrium conditions,

i.e., data taken after about 10 minutes at each bias value. When the probe indicates a voltage difference between the interconnects and the glass of about 500 volts, discharges occur spontaneously. These discharges cause the bias power supply to dip towards zero momentarily and cause transients on the beam current monitors inside the chamber. Discharges did not occur when positive bias voltages were applied. Attempts to measure the actual surface voltage profiles before and after discharges were not successful. These breakdowns appear to be similar to phenomena that occurs when solar array interconnects are biased negatively in the presence of a low energy thermal plasma environment.^{27,28-32} In this case, the interconnect potentials are also confined to the gap region but the breakdown threshold is plasma density dependent.

Analytical Results

An analytical modeling study was conducted to determine if the phenomena observed could be predicted. The study used the NASA Charging Analyzer Program (NASCAP) which is a three dimensional computer code that computes surface voltages of insulators and conductors exposed to charged-particle environments. The code has been described in the literature.³³

The model used in this study is shown in Fig. 4(a). It represents six solar cells (2x2 cm) with metallic interconnects modeled as wedges all mounted on Kapton substrate. Each computational cube shown is 4 mm on a side. This means that the gaps between the solar cells and the depth from the glass to interconnects are larger than actual. Several different model runs were made with the gap to depth ratio changed to verify that the results stated below were not changed by model geometry.

The predicted surface voltage profiles for a 4 keV electron beam irradiation of the solar cells are shown in Fig. 4(b) for three different bias voltages. The Kapton properties used were the same as those used in previous studies,³⁴ the interconnects were the NASCAP standard silver properties and the magnesium fluoride coatings on the solar cells had properties derived from recent preliminary results.²⁶

In the zero volt bias test, the center cell surface potential is predicted to be about -200 volts which compares reasonably well with the experimental data. The interconnect potential profile shows a trend to be confined to the gap region and is a positive gradient relative to the cover slides. The influence of the charging of the Kapton can also be seen here. The equipotential lines emanating from the highly charged Kapton tend to billow into space in front of the glass, setting up a barrier which, in this case, is approximately -300 volts; the potentials decay from the -300 volt line to zero volts at infinity. The charged Kapton forces the stronger voltage gradient shown in the right hand cells.

When the bias voltage is increased to -1.5 kV, the cover slide surface voltage is predicted to be about -1.2 kV which agrees with the -1.3 kV measured in the tests. The gradient in the gap is now negative; the cover glass is positive with respect to the interconnects. Note the establishment of the strong gradient on the right hand cell due to the bias voltages and the charging of the Kapton. The barriers seem to exist over the cover glass only.

At the -2.5 kV bias condition the predicted solar cell surface voltage is driven to about -1.8 kV. This compares well with the -1.6 kV found in the experiments. The gap voltage gradients are now indicated to be much more intense. The gradients at both the left and right hand cell edges have also become more severe.

The analysis conducted does predict values that agree with the experimental results. These predictions give a more detailed representation of the gradients that exist around the individual solar cells. It is possible that the discharges could be triggered within the interconnect gaps. Another possible discharge site is at the solar cell-insulator interface since the analysis indicates that gradients can be even more severe there. The conductor at the base of the cell could be exposed to the environment.

Satellite Behavior in Substorm Environments

The laboratory simulations have indicated that, when voltage gradients in the interconnect gap exceeds 500 volts (interconnect voltage negative with respect to cover slides), discharges can occur. In order to find out whether or not such a condition could occur on a satellite exposed to substorm environments, a satellite analytical study was conducted. In this study the NASCAP code was used on a model of a three-axis stabilized satellite. This satellite model (see Fig. 5(a)) has two solar array wings (1.8x3.0 m each) attached to a central spacecraft body. Dielectric materials used are shown on the figure. This model has been used in previous satellite behavior studies.¹⁴

This model was exposed to a design environmental specification for geomagnetic substorms.³⁵ Both sunlit and eclipse charging were studied for substorms characterized by the following two sets of conditions:

1. Moderate substorm - Electron Temperature of 8 keV, Electron Density of 2.1 cm^{-3} , Ion Temperature of 21 keV and Ion Density of 0.7 cm^{-3} .
2. Severe substorm - Electron Temperature of 11 keV, Electron Density of 1.1 cm^{-3} , Ion Temperature of 11 keV and Ion Density of 0.4 cm^{-3} .

During the sunlit charging simulation, sunlight was assumed to be at a 27° angle of incidence to the solar array wing.

The differential voltages developed during these substorm encounters on one of the solar array wings are shown in Fig. 5(b). The differentials on the other wing are similar to those shown. These voltages are the difference between the solar array covers (assumed to have high secondary yield magnesium fluoride coatings) and the array interconnects (assumed to be at 25 volts relative to the spacecraft body). The cover slides are less negative than the interconnects voltage. The curve marked base is for the region of the array next to the spacecraft body. As can be seen from these curves, differential charging takes a finite time to develop (on the order of a minute) in both sunlit and eclipse charging. In the sunlit charging simulation, the base region of the array is predicted to just reach the 500 volt breakdown criteria after 10 minutes in the moderate substorm environment. However, in the severe substorm sunlit charging simulation, both the base and central regions of the array could exceed the breakdown criteria. In eclipse charging the whole array could exceed the criteria within two minutes even in the moderate substorm.

Hence, it appears that conditions found in laboratory simulations for low differential voltage breakdowns in solar cell segments can exist on satellites encountering geomagnetic substorms. In sunlit charging simulations the breakdown criteria is predicted to be exceeded in severe substorms while the criteria is easily exceeded in eclipse charging. These results are encouraging for substantiating the basic concept, but there is still more to be done to understand this breakdown mechanism and its relation-

ship to satellite breakdowns. Additional parametric studies in laboratory are required and studies of different types of satellites in various environmental conditions must be done before definitive statements on this mechanism can be made.

Concluding Remarks

Space data from the P78-2, SCATHA, satellite has shown that differential charging of shaded insulators relative to the structure potential is limited to values of about 3 kV. Analytical modeling studies of various satellite configurations exposed to reasonable geomagnetic substorm environments have confirmed this limitation. It had been believed that differential charging was responsible for triggering discharges that were responsible for the anomalies observed in geosynchronous satellite systems. Based on ground simulation results, discharges required differential voltages of about 10 kV to be initiated. From these two pieces of information one would be led to believe that no discharges would occur on satellites. Yet, discharges do occur as evidenced by SCATHA data, by CTS harness noise counters and by other detectors. Therefore, other mechanisms to generate discharges have to be postulated and evaluated. One possibility is to assume that the discharges could be triggered by positive voltage gradients in the gaps between the solar cells on arrays.

The basic concept in this solar array gap breakdown postulation is that solar array cover slides are at a less negative voltage than the interconnects. This means that the interconnect will be negative (a possible cathode) with respect to the cover slides. It is possible then to imagine that the gradients could build up in the gap to a point where discharges could be triggered.

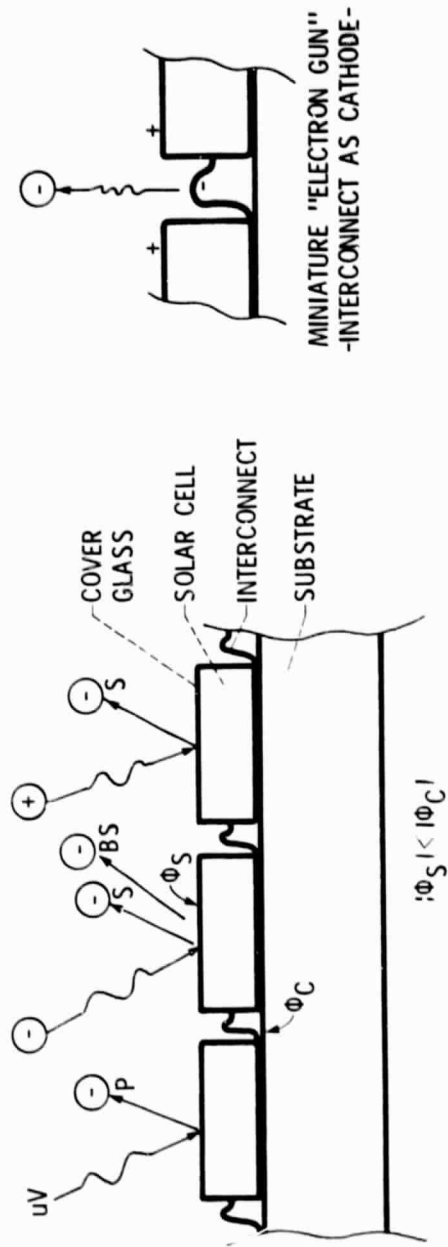
This concept was investigated both analytically and experimentally. The experiment used a 24 cell solar array segment in which the interconnects were biased to both positive and negative voltages by a power supply while the cover slides were irradiated with monoenergetic electrons. The results indicated that discharges would occur only when the surface voltage probe indicated that the cover slides were 500 volts less negative than the interconnects. The analytical modeling of a segment in similar conditions verified the development of strong electric fields in the gap regions and also indicated the development of strong electric fields at the interconnect-glass-substrate interface.

An analytical modeling study of a satellite in a design criteria environment was conducted to determine if the 500 volt differential could be met or exceeded. For the three-axis stabilized satellite model considered, it was found that regions of the array would exceed the 500 volt differential under sunlit charging in a severe environment and would exceed this value under moderate substorm environments in eclipse charging. Hence, it is concluded that this is a possible mechanism for producing discharges on geosynchronous satellites.

References

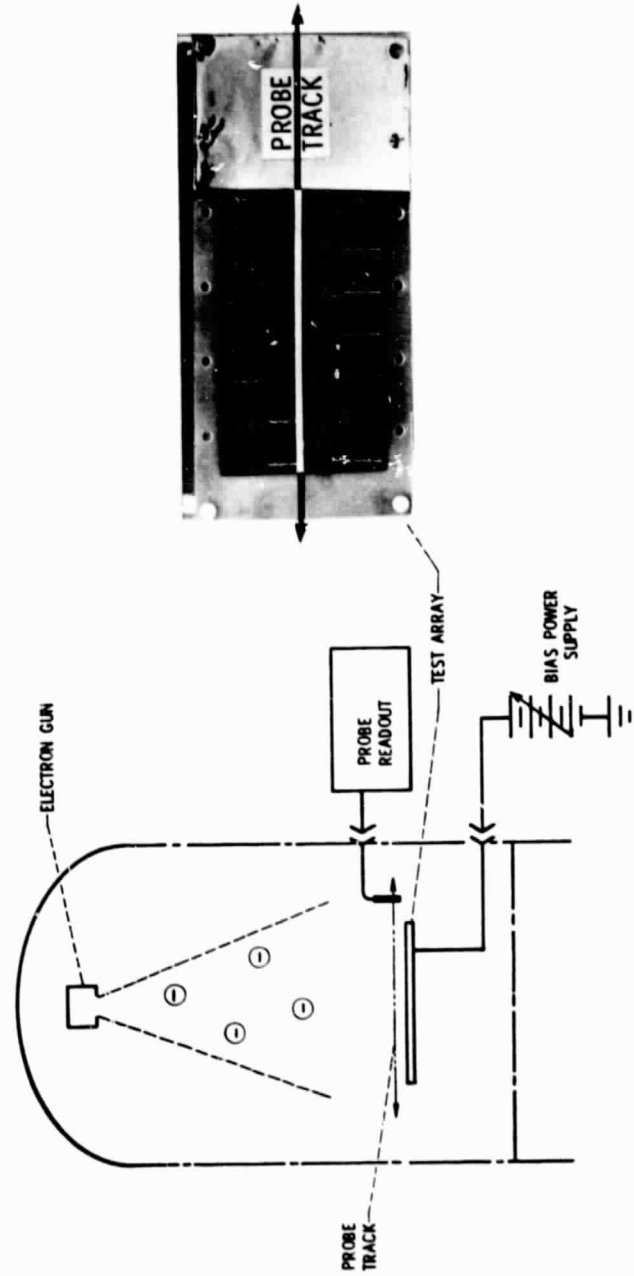
1. McPherson, U. A., Cauffman, U. P., and Schober, W., "Spacecraft Charging at the High Altitudes - The SCATHA Satellite Program," Spacecraft Charging By Magnetospheric Plasmas, Progress in Astronautics and Aeronautics, Vol. 47, A. Rosen, ed. American Institute of Aeronautics and Astronautics, New York, 1976, pp. 15-30.
2. Ueferost, S. E. and McIlwain, C. E., "Plasma Clouds in the Magnetosphere," Journal of Geophysical Research, Vol. 76, June 1971, pp. 3587-3611.

3. DeForest, S. E., "Spacecraft Charging at Synchronous Orbit," Journal of Geophysical Research, Vol. 77, Feb. 1972, pp. 651-659.
4. Stevens, N. J., Lovell, R. R., and Gore, V., "Spacecraft Charging Investigation for the CTS Project," Spacecraft Charging by Magnetospheric Plasmas, Progress in Astronautics and Aeronautics, Vol. 47, A. Rosen, ed., American Institute of Aeronautics and Astronautics, New York, 1976, pp. 263-275.
5. Olsen, R. C., Whipple, E. C., and Purvis, C. K., "Active Modification of ATS-5 and ATS-6 Spacecraft Potentials," Proceedings of the 1978 Symposium on the Effect of the Ionosphere on Space and Terrestrial Systems, Naval Research Laboratory, Washington, DC, 1978, pp. 328-336.
6. Stevens, N. J., Berkopce, F. D., Staskus, J. V., Blech, R. A., and Narciso, S. J., "Testing of Typical Spacecraft Materials in a Simulated Substorm Environment," Proceedings of the Spacecraft Charging Technology Conference, C. P. Pike and R. R. Lovell, eds., NASA TM X-73537/AFGL TR-77-0051, 1977, pp. 431-457.
7. Belanger, V. J. and Eagles, A. E., "Secondary Emission Conductivity of High Purity Silica Fabric," Proceedings of the Spacecraft Charging Technology Conference, C. P. Pike and R. R. Lovell, eds., NASA TM X-73537/AFGL TR-77-0051, 1977, pp. 655-686.
8. Balmain, K. G., "Scaling Laws and Edge Effects for Polymer Surface Discharges," Spacecraft Charging Technology - 1978, NASA CP-2071/AFGL TR-79-0082, 1979, pp. 646-656.
9. Inouye, G. T., Sanders, N. L., Komatsu, G. K., Valles, J. R., and Sellen, J. M., Jr., "Thermal Blanket Metallic Film Groundstrap and Second Surface Mirror Vulnerability to Arc Discharges," Spacecraft Charging Technology - 1978, NASA CP-2071/AFGL TR-79-0082, 1979, pp. 657-681.
10. Aron, P. R. and Staskus, J. V., "Area Scaling Investigations of Charging Phenomena," Spacecraft Charging Technology - 1978, NASA CP-2071/AFGL TR-79-0082, 1979, pp. 485-506.
11. Mizera, P. F. and Boyd, G. M., "Satellite Surface Potential Survey," Spacecraft Charging Technology - 1980, NASA CP-2182, 1981, pp. 461-469.
12. Inouye, G. T., "Spacecraft Potentials in a Substorm Environment," Spacecraft Charging by Magnetospheric Plasmas, Progress in Astronautics and Aeronautics, Vol. 27, A. Rosen, ed., American Institute of Aeronautics and Astronautics, New York, 1976, pp. 103-120.
13. Sanders, N. L. and Inouye, G. T., "NASCAP Charging Calculations for a Synchronous Orbit Satellite," Spacecraft Charging Technology - 1980, NASA CP-2182, 1981, pp. 684-708.
14. Stevens, N. J., "Analytical Modeling of Satellites in Geosynchronous Environment," Spacecraft Charging Technology - 1980, NASA CP-2182, 1981, pp. 717-729.
15. Mandell, M. J., Katz, I., Schneulle, G. W., Steen, P. G., and Roche, J. C., "The Decrease in Effective Photocurrents due to Saddle Points in Electrostatic Potentials near Differentially Charged Spacecraft," IEEE Transactions on Nuclear Science, Vol. NS-25, Dec. 1978, pp. 1313-1317.
16. Shaw, R. R., Nanevich, J. E., and Adamo, R. C., "Observations of Electrical Discharges Caused by Differential Satellite Charging," Spacecraft Charging by Magnetospheric Plasmas, Progress in Astronautics and Aeronautics, Vol. 47, A. Rosen, ed., American Institute of Aeronautics and Astronautics, New York, 1976, pp. 61-76.
17. Stevens, N. J., Klinefelter, V. W., and Gore, J. V., "Summary of CTS Transient Event Counter Data After One Year of Operation," IEEE Transactions on Nuclear Science, Vol. NS-24, Dec. 1977, pp. 2270-2275.
18. Koons, H. C., "Aspect Dependence and Frequency Spectrum of Electrical Discharges on the P78-2 (SCATHA) Satellite," Spacecraft Charging Technology - 1980, NASA CP-2182, 1981, pp. 478-492.
19. Meulenbergh, A., Jr., "Evidence for a New Discharge Mechanism for Dielectrics in a Plasma," Spacecraft Charging by Magnetospheric Plasmas, Progress in Astronautics and Aeronautics, Vol. 47, A. Rosen, ed., American Institute of Aeronautics and Astronautics, New York, 1976, pp. 237-246.
20. Frederickson, A. R., "Bulk Charging and Breakdown in Electron-Irradiated Polymers," Spacecraft Charging Technology - 1980, NASA CP-2182, 1981, pp. 33-51.
21. Flanagan, T. M., Denson, R., Mallon, C. E., Treadaway, M. J., and Wenaas, E. P., "Effect of Laboratory Simulation Parameters on Spacecraft Dielectric Discharges," IEEE Transactions on Nuclear Science, Vol. NS-26, Dec. 1979, pp. 5134-5140.
22. Reddy, J., "Electron Irradiation Tests on the European Meteorological Satellite," Spacecraft Charging Technology - 1980, NASA CP-2182, 1981, pp. 835-855.
23. Staskus, J. V. and Roche, J. C., "Testing of a Spacecraft Model in a Combined Environment Simulator," to be presented at 1981 IEEE Annual Conference on Nuclear and Space Radiation Effects, Seattle, WA, July 21-24, 1981.
24. Inouye, G. T., Sellen, J. M., Jr., "TURSS Solar Array Arc Discharge Tests," Spacecraft Charging Technology - 1978, NASA CP-2071/AFGL TR-79-0082, 1979, pp. 834-852.
25. Stang, D. B. and Purvis, C. K., "Comparison of NASCAP Modeling Results with Lumped-Circuit Analysis," Spacecraft Charging Technology - 1980, NASA CP-2182, 1981, pp. 665-683.
26. Krainsky, I., Lundin, W., Gordon, W. L., and Hoffman, K. W., "Secondary Electron Emission Yields," Spacecraft Charging Technology - 1980, NASA CP-2182, 1981, pp. 179-197.
27. Stevens, N. J., "Solar Array Experiments on the SPHINX Satellite," NASA TM X-71458, 1973.
28. Herron, B. G., Bayless, J. R., and Worden, J. D., "High Voltage Solar Array Technology," AIAA Paper 72-443, Apr. 1972.
29. Kennerud, K. L., "High Voltage Solar Array Experiments," Boeing Aerospace Co., Seattle, WA, Mar. 1974 (NASA CR-121280).
30. Domitz, S. and Grier, N. T., "The Interaction of Spacecraft High Voltage Power Systems with the Space Plasma Environment," PESC '74 Record, Proceedings of the Power Electronics Specialists Conference, Institute of Electrical Engineers, Inc., New Jersey, 1974, pp. 62-69.
31. Stevens, N. J., Berkopce, F. D., Purvis, C. K., Grier, N. T., and Staskus, J. V., "Investigation of High Voltage Spacecraft System Interactions with Plasma Environments," AIAA Paper 78-672, Apr. 1978.
32. Grier, N. T., "Experimental Results on Plasma Interactions with Large Surfaces at High Voltages," NASA TM-81423, 1980.
33. Katz, I., Cassidy, J. J., Mandell, M. J., Schneulle, G. W., Steen, P. G., and Roche, J. C., "The Capabilities of the NASA Charging Analyzer Program," Spacecraft Charging Technology - 1978, NASA CP-2071/AFGL TR-79-0082, 1979, pp. 101-122.
34. Purvis, C. K. and Staskus, J. V., "Scatha SSPM Charging Response: NASCAP Predictions Compared with Data," Spacecraft Charging Technology - 1980, NASA CP-2182, 1981, pp. 592-607.
35. Stevens, N. J., "Use of Charging Control Guidelines for Geosynchronous Satellite Design Studies," Spacecraft Charging Technology - 1980, NASA CP-2182, 1981, pp. 789-801.



(a) Solar cell configuration.

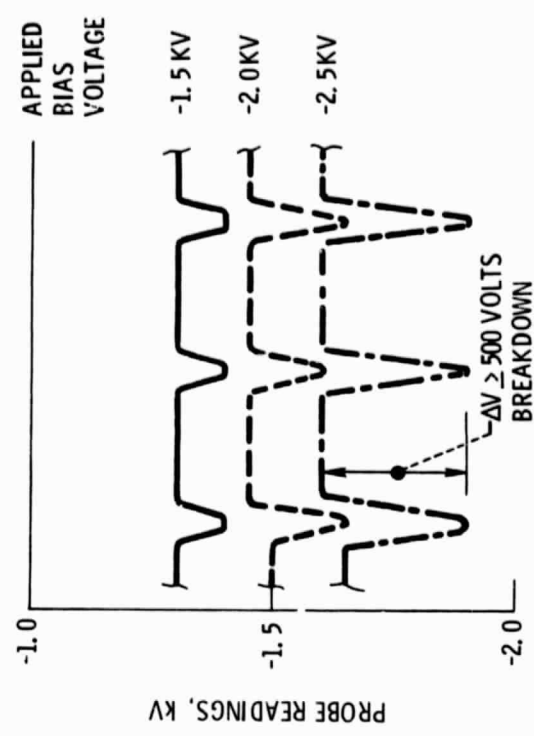
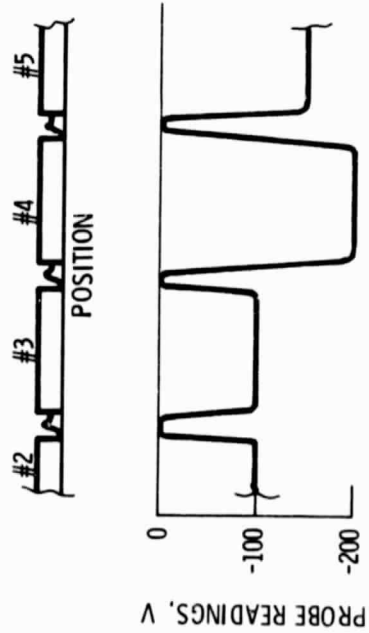
Figure 1. - Voltages on solar arrays.



(a) Bell jar vacuum system schematic.

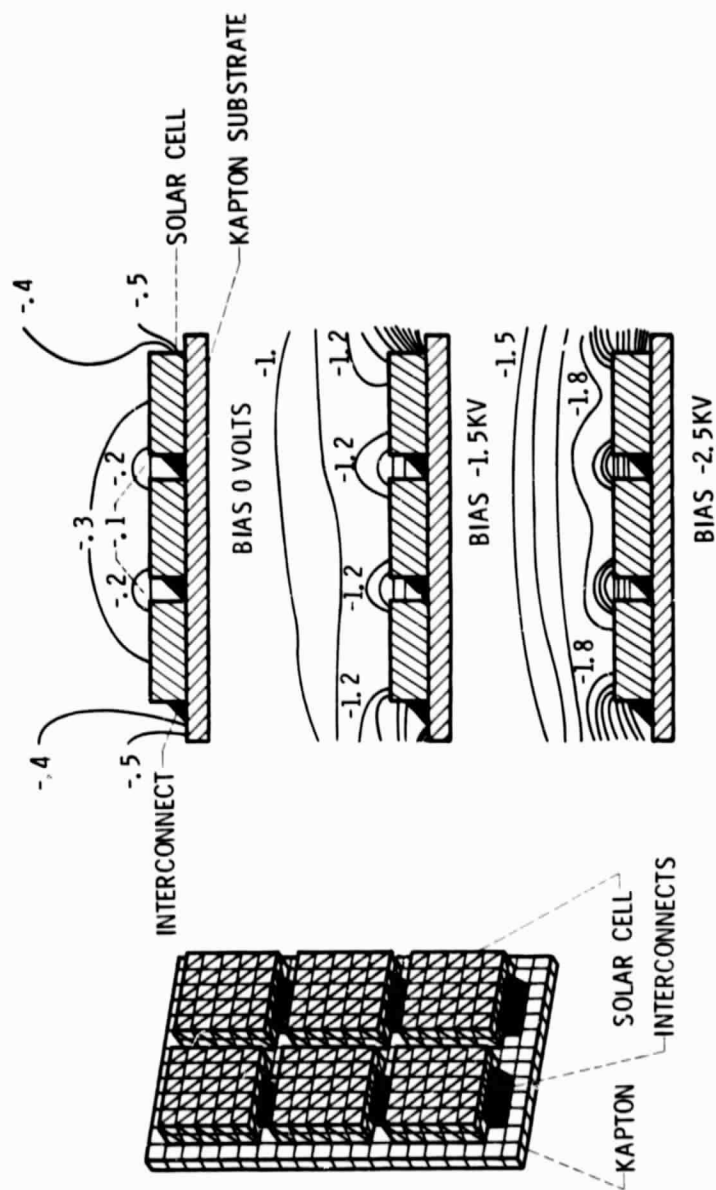
(b) Solar array segment.

Figure 2. - SAGES experimental arrangement



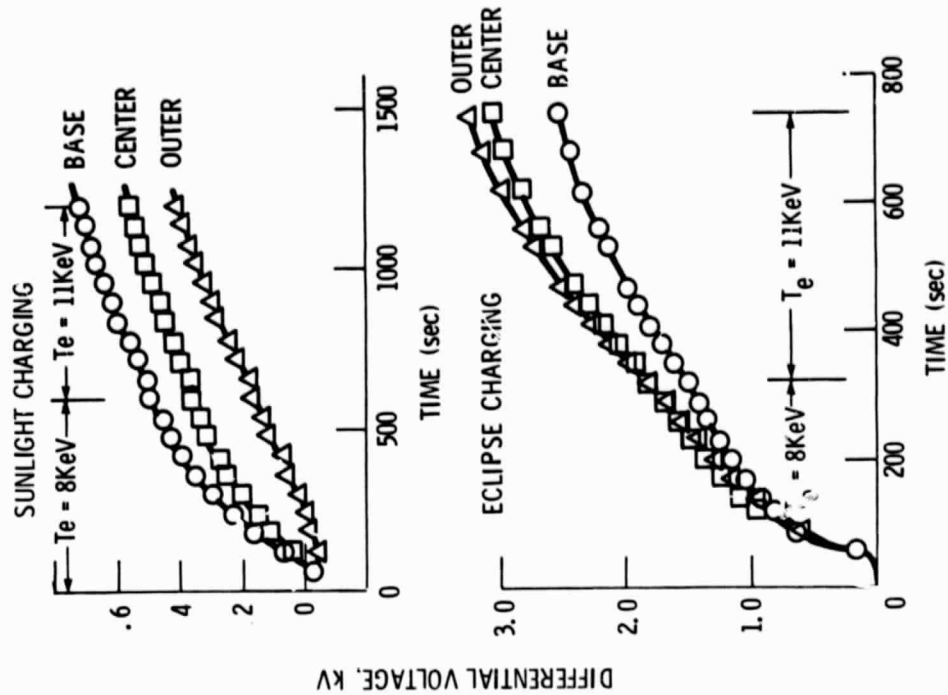
(a) Interconnects grounded. (b) Interconnects biased.

Figure 3. - Experimental results - solar array voltages; 4 keV electron beam.



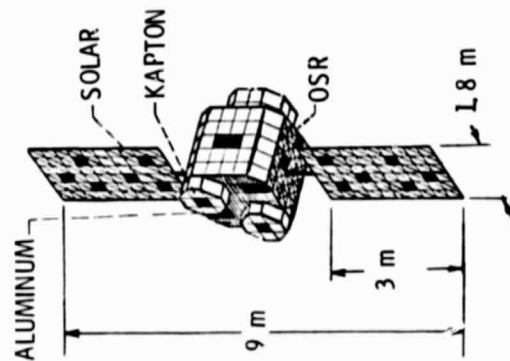
(a) NASCAP model. (b) Predicted potential profiles; 100-volt equipotentials.

Figure 4. - Predicted solar array segment potentials.



(a) NASCAP model.

(b) Substorm differential charging.



(a) NASCAP model.

(b) Substorm differential charging.

Figure 5. - Satellite solar array differential charging.